Star cracks in continuously cast peritectic steel slabs

M. Herrera-Trejo*[1], J. J. Ruiz[1], M. Castro-Roman[1] and H. Solis[2]

This work consisted of the characterisation of star cracks found on the surface of continuously cast steel slabs solidification experiments on molten steel in Cu moulds, with and without ceramic insulation. Cracks located at the slab surface were propagated through the grain boundaries, with the presence of Cu particles observed along the crack paths. Zones normal to the cracks exhibited an iron oxide layer followed by Cu particles and the steel matrix. Specimens solidified in Cu moulds showed an iron oxide/Cu/steel layer arrangement extending from the sample surface towards the steel matrix, as well as a penetration of Cu through the grain boundaries. In contrast, in samples solidified in ceramic insulated Cu moulds, Cu particles were neither observed at the surface nor at the grain boundaries. Thus, it is thought that the star cracks are due to liquid steel/Cu mould interaction during casting and that they are formed during primary cooling in the mould in the continuous casting machine and then they propagate during secondary cooling and bending operations. It is also thought that cracking susceptibility is promoted by peritectic transformation which occurs at high solid fractions.

Keywords: Star cracks, Solidificaction, Surface defect, Steel, Peritectic

Introduction

Cast slabs frequently exhibit surface defects that are associated with severe cooling conditions during solidification in the continuous casting mould. Additionally, thermal and mechanical stresses produced during secondary cooling and slab bending operations also promote the generation of surface defects.[1–4]

One type of surface defect found in slabs is the so called star crack.[5] This defect is revealed after the slab surface oxide layer has been removed by scarfing. This operation increases the surface temperature and so the crack's nature is altered, causing loss of evidence that could help explain its formation mechanism.

This type of crack is associated with the presence of Cu, which could come either from the steel or from the continuous casting mould.[5–8] When Cu content in the slab exceeds its solubility in austenite,[6] liquid Cu precipitates at the steel surface during the oxidation at high temperatures, resulting in the penetration of Cu into the grain boundaries.

On the other hand, liquid steel/Cu mould interaction is not well understood; the mechanisms that have been proposed for the formation of these kinds of cracks are based on studies focused on the description of steel–Cu interaction. In these studies, contact between solid steel and liquid Cu is promoted under isothermal conditions for relatively long times. Under such conditions, the proposed crack formation mechanism is associated with the presence of liquid Cu at the steel grain boundaries and triple points.[6,7] However, the conditions under which this information has been obtained differ significantly from those observed in the continuous casting mould.

This work presents the characterisation results of star cracks found in industrially produced steel slabs. Additionally, solidification experiments on molten steel were carried out in order to elucidate the source of Cu, i.e. whether it is associated with the liquid steel/Cu mould interaction and/or with Cu precipitation during oxidation processes at high temperatures.

Experimental procedure

The experimental procedure employed basically consisted of two stages: characterisation of star cracks found in industrially produced steel slabs, and solidification experiments on molten steel in both Cu moulds, and Cu moulds with ceramic insulation.

Characterisation of star cracks

The visual observation of the cracks found in steel slabs having the chemical composition of 0·13C–1·15Mn–0·01P–0·005S–0·15Si–0·035Al–0·15Cu–0·06V (wt-%), was carried out after conducting a scarfing operation on the entire surface of the slabs. Typical defects were carefully extracted from the steel slabs by cutting off small steel pieces that contained them, avoiding an excessive heating of areas very close to the cracks. Characterisation of the latter defects began with an

[1]Cinvestav Saltillo, Ramos Arizpe, Coahuila, Mexico
[2]Ternium de México SA de CV, San Nicolás de los Garza, NL, Mexico

*Corresponding author, email martin.herrera@cinvestav.edu.mx

Published by Maney on behalf of the Institute
Received 5 September 2008; accepted 18 March 2009
DOI 10.1179/174328109X445651

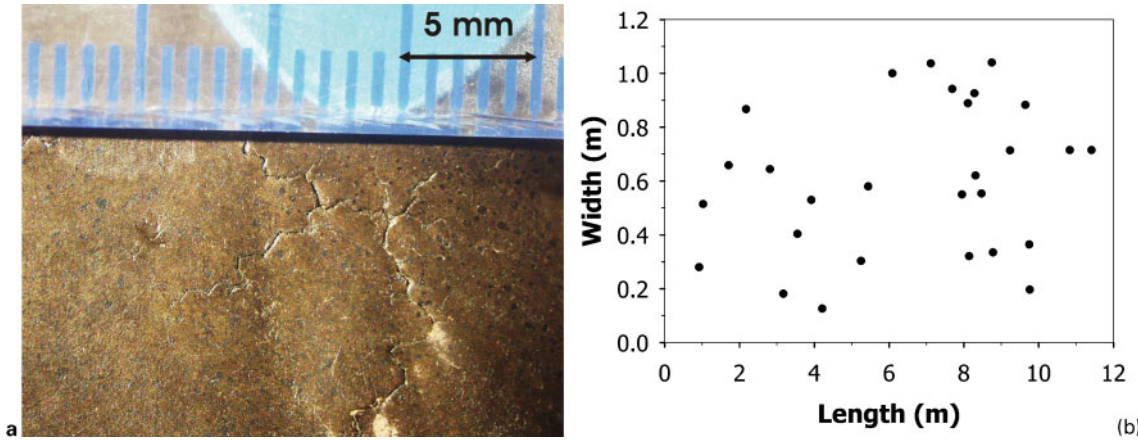

1 ***a*** **representative star crack and** ***b*** **location of cracks at inferior surface of steel slabs**

analysis of the slab surface that was exposed after the scarfing operation. Subsequently, the surfaces generated by propagation of the cracks were separated and analysed using a scanning electron microscope (SEM). In order to obtain information on regions adjacent to the surfaces generated by crack propagation, the samples containing these surfaces were perpendicularly cut and the resulting surfaces were metallographically prepared and analysed with SEM. The metallographic preparation consisted of a series of conventional grinding and polishing steps.

Solidification experiments

In order to obtain information on liquid steel/Cu mould interaction under similar cooling conditions to those found in the continuous casting mould, liquid steel was poured into Cu moulds. With the objective of elucidating whether the presence of Cu can be attributed to its precipitation during the oxidation processes at high temperatures, additional solidification experiments were conducted in Cu moulds with ceramic insulation, to avoid liquid steel/Cu mould interaction during solidification.

For these experiments, liquid steel was poured into cylindrical Cu moulds of 3 cm diameter and 7 cm height, this way promoting radial rather than axial heat flow. A mould wall thickness of 2 cm allowed achievement of a cooling rate similar to that reported for zones near the surface of industrially cast conventional steel slabs.[9] Each Cu mould was fitted with a type B thermocouple in order to record the thermal evolution and to estimate cooling rate during solidification of the samples. The thermocouple was placed close to the mould wall and suspended at mid mould height; it was connected to a computerised data acquisition system.

The steel employed was from the same steel slab from which the crack containing specimens were cut. In order to carry out the solidification tests, 12 kg steel were melted in an induction furnace using prefusion slag as protecting cover for the liquid bath. Then, the liquid steel was poured at 1600°C into the Cu moulds. The solidified samples were cross-sectioned in a plane passing by the tip of the thermocouple and analysed with SEM at a region close to the surface that made contact with the mould wall. In order to carry out these analyses, the samples were previously prepared metallographically.

Results and discussion

Characterisation of star cracks

Figure 1*a* shows a representative star crack found at the surface of the steel slab. Figure 1*b* illustrates the location of this type of defect in the entire inferior surface of the sampled slab, showing a random distribution of these defects. Figure 2 shows a crack surface, revealing a crack propagation path opposite the heat extraction direction. The propagation path followed the grain boundaries, showing angular and smooth surfaces typical of brittle fractures.[10–12] The analysis of the crack surface at higher magnifications revealed the presence of bright particles, as shown in Fig. 3*a*, which contained Cu according to the energy dispersive spectrometry (EDS) spectrum shown in Fig. 3*b*.

The concentration profiles obtained by SEM/EDS at a surface perpendicular to the crack surface (Fig. 4), indicated the presence of an iron oxide layer, which was followed by Cu particles and the steel matrix. This showed that Cu is not present in the steel grains, and thus its presence is confined to the sample surface and nearby regions.

Solidification experiments

Thermal analyses

Figures 5*a* and *b* shows representative temperature evolution of samples solidified in Cu moulds with and without ceramic insulation respectively. The application

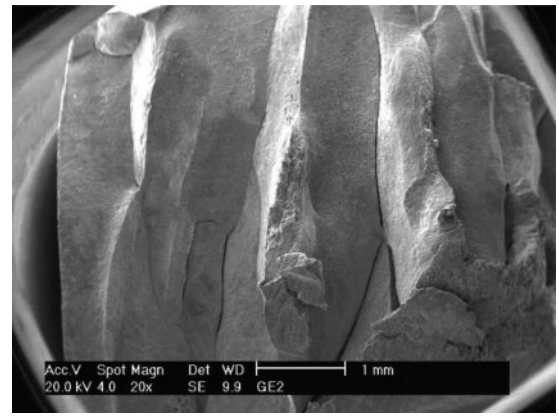

2 Crack surface

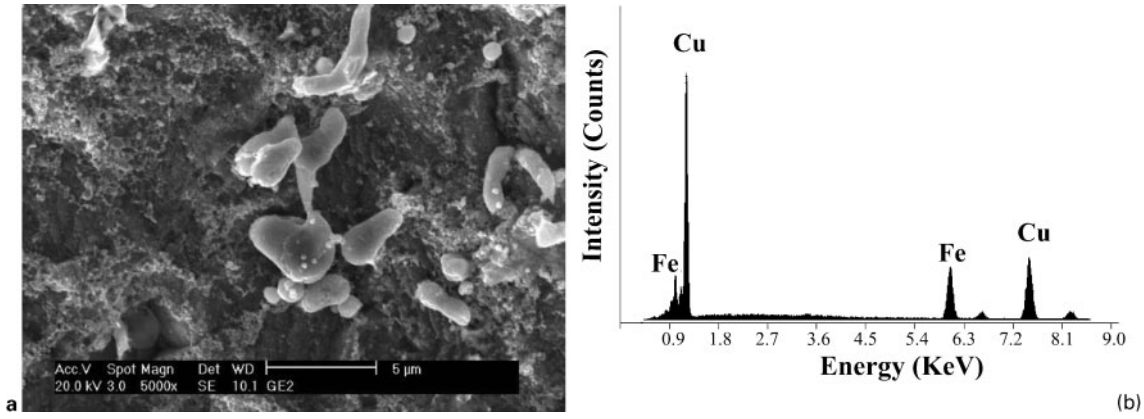

3 ***a*** **particles on crack surface and** ***b*** **EDS spectrum of latter particles**

of a procedure developed by Alfaro,[13] based on the derivative thermal analysis technique, allowed to determine initial and final solidification temperature. Based on these data, solidification time (time elapsed in the solid–liquid region) was determined and hence the cooling rate was estimated by dividing the difference between initial and final solidification temperature by the solidification time. Cooling rates of 6 and 21 K s^{-1} were obtained for the solidified steel in Cu mould with and without ceramic insulation respectively. It is noteworthy that the cooling rate of 21 K s^{-1} is of the same magnitude order as those reported by Louhenkilpi *et al.*[9] for areas close to the surface of conventional steel slabs produced by continuous casting.

Characterisation of solidified steel samples

For solidified steel in Cu mould, Fig. 6*a* and *b* shows SEM images obtained at the surface that was in contact with the Cu mould and at its adjacent zone. In both cases, bright particles located at the grain boundaries and at the sample surface, as well as dark zones located at the latter surface, were observed. The bright particles were constituted by Cu, as can be observed in the corresponding EDS spectrum shown in Fig. 6*c*, whereas the dark zones located at the sample surface corresponded to iron oxide, according to the EDS spectrum shown in Fig. 6*d*. It is worth mentioning that the maximum penetration depth at which Cu was found at the grain boundaries was 20 μm. Figure 7 shows a chemical profile obtained at the region adjacent to the sample surface. This figure shows the presence of an iron oxide layer located at the sample surface, followed progressively by a Cu layer and the steel matrix. Also, Fig. 7 shows that Cu is absent at the interior of the steel grains.

On the other hand, in relation to steel samples solidified in Cu moulds with ceramic insulation, Fig. 8 shows a SEM image obtained from a zone adjacent to the surface that was in contact with the ceramic insulator. In this figure, EDS spectrums are included which were obtained from three different zones indicated in the micrograph. An arrangement was observed, consisting of an iron oxide superficial layer followed by a layer of iron–silicon oxides and the steel matrix.

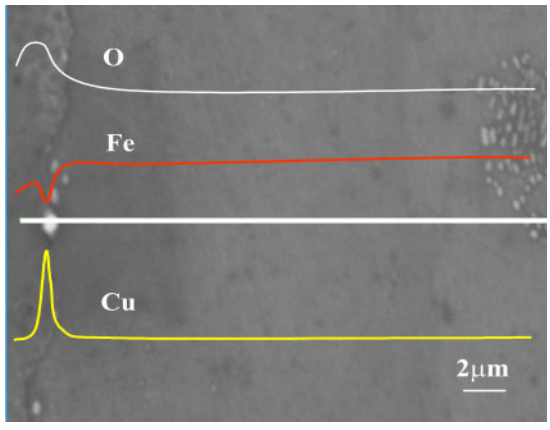

4 Concentration profiles starting at crack surface

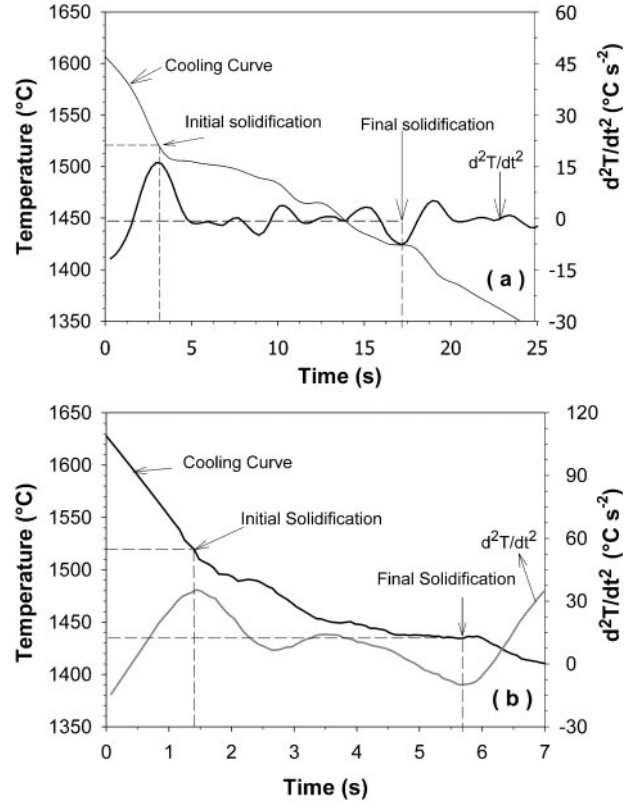

5 Representative temperature evolution of samples solidified in Cu moulds ***a*** **with and** ***b*** **without ceramic insulation**

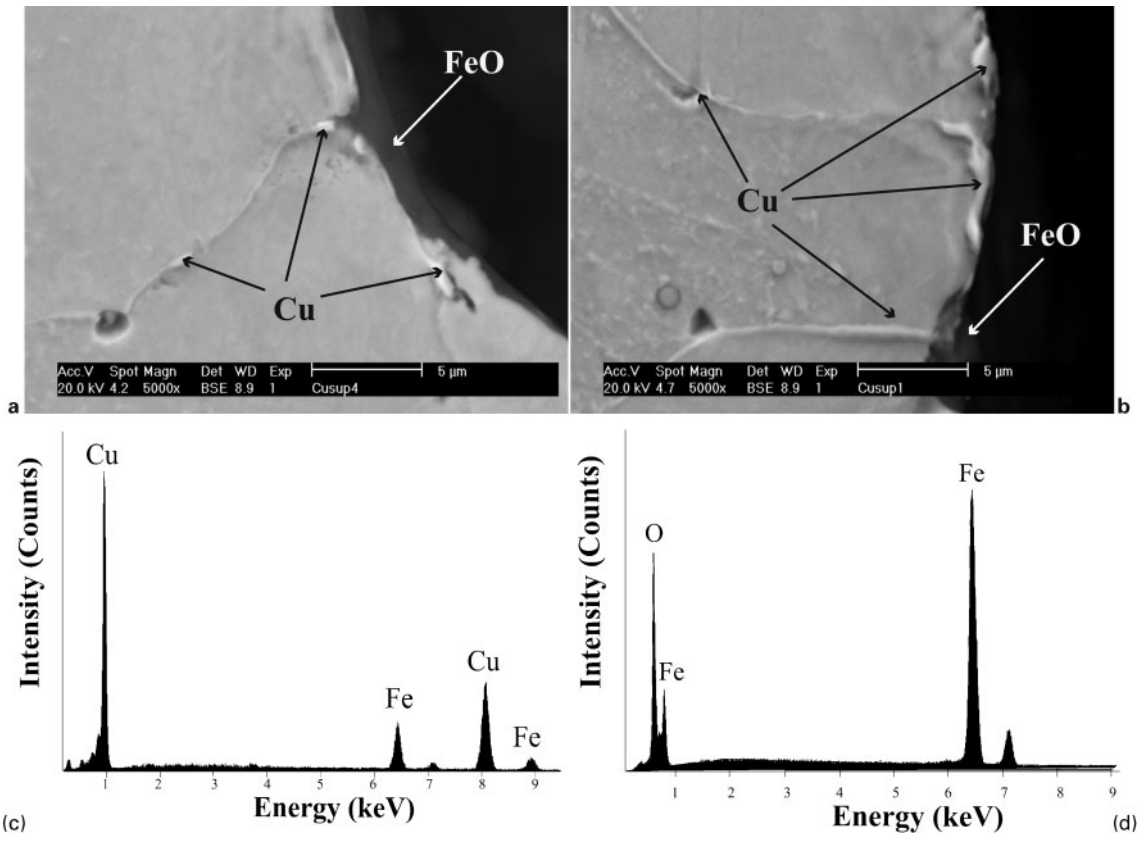

6 ***a,b*** **penetration of Cu into steel grain boundaries;** ***c,d*** **EDS spectra for light particles and dark zones respectively**

Discussion

The observations made on the solidified samples in Cu moulds, i.e. Cu particles at the surface of the samples and Cu penetration into the grain boundaries, as well as the absence of Cu in the solidified samples in Cu moulds with ceramic insulation, suggest that Cu found in solidified samples comes from the liquid steel/Cu mould interaction. Therefore, considering the magnitude of the cooling rate that was reached in the solidification experiments, 21 K s^{-1}, it is assumed that this mechanism operates during the surface solidification of steel slabs in continuous casting.

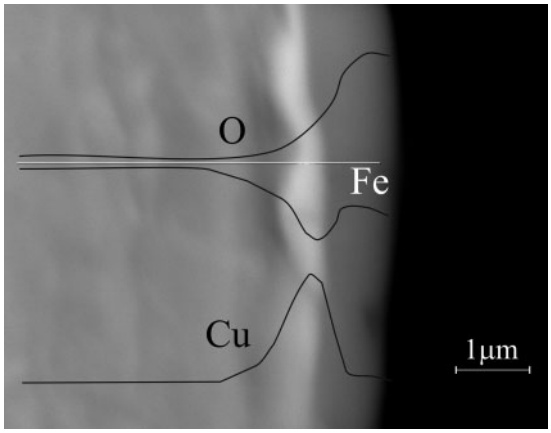

7 Concentration profile starting at surface of sample obtained in solidification test

Mizukami *et al.*[14] and Ruiz *et al.*[15] have shown that steels of peritectic composition exhibit cracking susceptibility toward the end of solidification, which is dependent on the fraction of the phases. Hence, the evolution of phases at cooling conditions similar to those found in continuous casting was simulated with the aid of DICTRA[16] (diffusion controlled transformations) software. Thus, the obtained cooling curve shown in Fig. 1 was introduced into the software in order to simulate the evolution of phases; details of the calculation are described in previous works by Ruiz *et al.*[15] Also, considering that differences in the mechanical behaviour of both phases δ and γ at high temperatures can induce strains at their interfaces with the consequent generation of cracks, the tensile strength and elongation of δ and γ phases were evaluated as a function of the solid fraction, using expressions given by Mizukami *et al.*[14]

Figure 9*a* shows the evolution of phases as a function of solid fraction. The fraction of δ phase increases until γ phase begins to form at a solid fraction of 0·85. Above this value, the fraction of δ phase decreases until it becomes equal to the fraction of γ phase at a solid fraction of 0·92. Then, δ phase disappears completely at a solid fraction of 0·98, and from this point onwards, additional quantities of γ phase are formed from the remaining liquid. Figure 9*b* and *c* shows the variation of the tensile strength and elongation of δ and γ phases as a function of solid fraction. It can be seen that, in the solid fraction range of 0·85–0·87, γ phase shows the lowest tensile strength and elongation values, which indicates that deformation occurs in this phase. In contrast, in the solid fraction range of 0·87–0·92, the tensile strength of

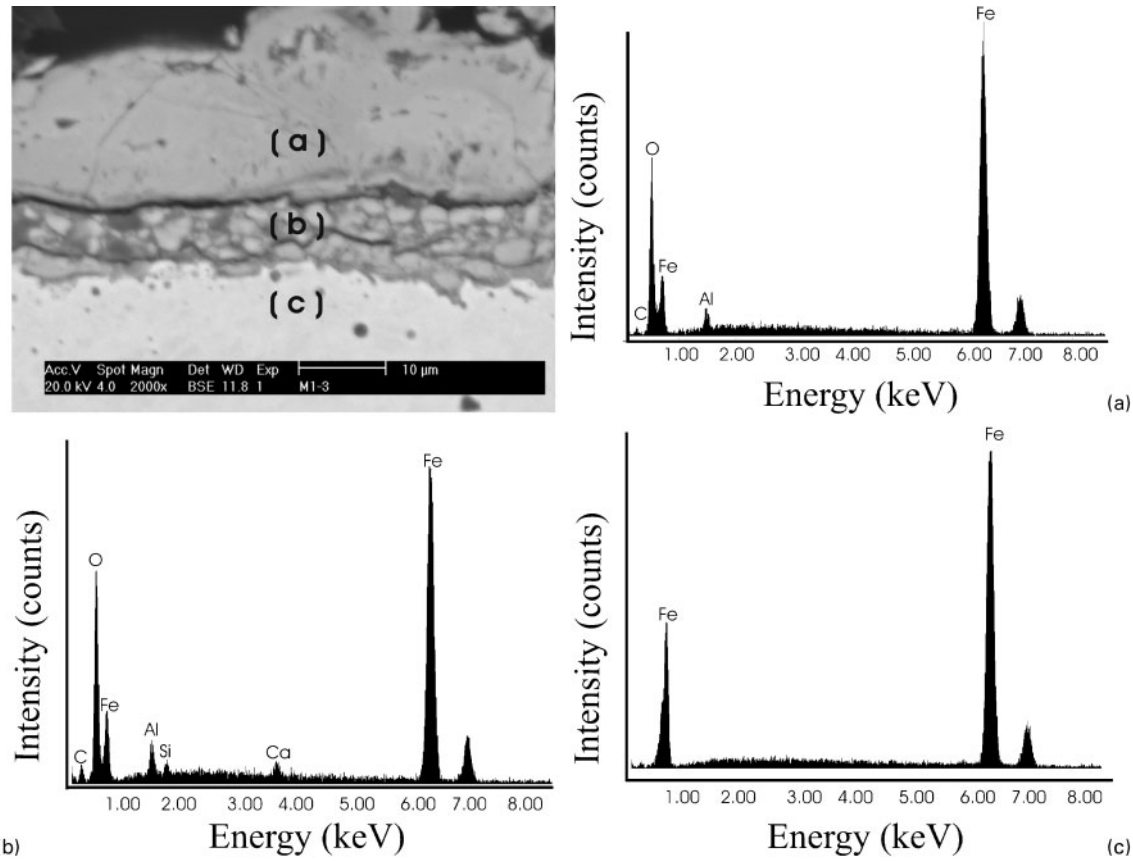

8 Micrograph obtained from adjacent to surface, and EDS spectra for zone indicated in micrograph

δ phase is lower than that of γ phase but the latter phase shows the lowest elongation value. Consequently, in this solid fraction range the deformation does not occur in any phase.

Above a solid fraction value of 0·92, at which ductility is equal for both δ and γ phases, the latter phase shows the highest ductility and tensile strength values. This indicates that in the solid fraction range of 0·92–0·98, deformation occurs in the δ phase. Thus, for the studied steel solidification conditions, the just mentioned tendencies take place at the solid fraction ranges of 0·85–0·87 and 0·92–0·98 (Fig. 9). This agrees well with the generally accepted hypothesis, which states that the formation of cracks begins in the meniscus zone during primary cooling, before the end of solidification.[2,4,8] In this context, it is thought that the differences in mechanical behaviour of the phases during the peritectic transformation, together with the weakening of their grain boundaries due to the penetration of Cu, contributed to the initial formation of the cracks that were found in the steel slabs.

Additionally, considering the criterion proposed by Clyne *et al.*,[17] which relates the incidence of cracking at solid fractions higher than 0·9, where the remaining liquid is unable to feed the contraction, it is thought that cracking susceptibility in the studied steel depends on the solid fraction range within which the peritectic transformations occurs. It is observed in Fig. 9 that only $\sim$0·5 of mass fraction of δ phase has transformed at 0·91 of solid fraction, which means that part of the contraction associated with the peritectic transformation is not fed by the remaining liquid.

On the other hand, in the analysed star cracks, the penetration of Cu towards the interior of the steel slab was more pronounced with respect to that observed in the solidification experiments. This suggests that the cracks that were initially formed in the continuous casting mould are subsequently propagated towards the interior of the steel slabs as a consequence of thermal and mechanical stresses generated during the secondary cooling stage, particularly at the inferior face of the steel slabs. During the propagation of the cracks that occurred at this stage, Cu is solid and is concentrated at an area close to the surface of the steel slabs, according to the iron oxide–Cu–steel matrix arrangement observed in Fig. 7. The presence of Cu at penetration depths much greater than those observed in the solidification experiments, 20 µm, can then be explained considering Cu melting during the surface scarfing operation followed by penetration of molten Cu into the crack by a capillary effect.

Conclusions

Characterisation of star cracks found at the surface of continuously cast steel slabs, together with an analysis of steel specimens solidified in Cu moulds with and without ceramic insulation, allowed us to draw the following conclusions.

1. Star cracks can be associated with liquid steel/Cu mould interaction, which promotes Cu penetration into the grain boundaries.

2. At a cooling rate of the same magnitude order as that estimated for zones close to the surface of

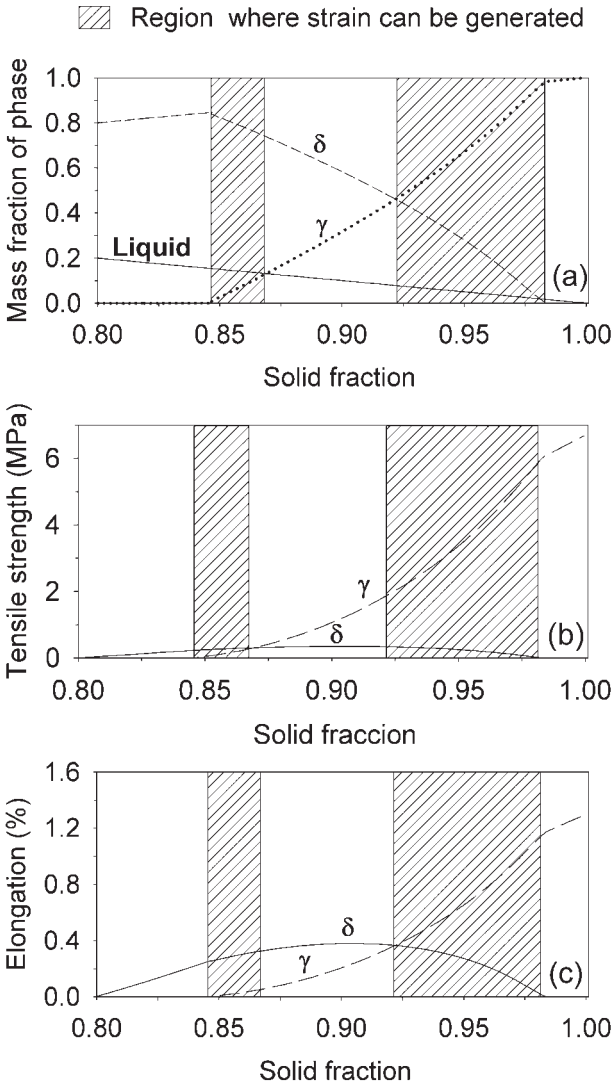

9 Relationship between *a* phase weight fraction, *b* tensile stress, *c* elongation, and solid fraction for peritectic steels

continuous cast steel slabs, Cu penetrates rapidly through the grain boundaries.

3. The presence of Cu at the surface cracks, together with the iron oxide/Cu/steel arrangement extending from the crack surface and the solidified sample surface towards the steel matrix, suggests that not only the star cracks are formed during primary cooling at the mould of a continuous casting machine, but also that they are subsequently propagated during both secondary cooling and bending operations.

Acknowledgement

The authors wish to extend their appreciation to the CONACYT and COECYT for their financial support.

References

1. W. R. I. A. A. Perkins: Proc. Int. Conf. on 'Basic parameters affecting the quality of continuously cast slabs', Biarritz, France, June 1976, The Metals Society, 330.
2. J. K. Brimacombe and K. Sorimachi: 'Continuous casting heat flow, solidification and crack formation', 199–213; 1984, New York, ISS of AIME.
3. W. R. Irving: 'Continuous casting steel', 207; 1993, England, The Institute of Materials.
4. H. Shibata, Y. Arai, M. Suzuki and T. Emi: *Metall. Trans. B*, 2000, **31B**, 981–991.
5. J. K Brimacombe, E. B. Hawbolt and F. Weinberg: 'Continuous casting heat flow, solidification and crack', 229–238; 1984, New York, ISS of AIME.
6. T. Kajitani, M. Wakoh, N. Tokumitsu, S. Ogibayashi and S. Mizoguchi: 'Influence of temperature and strain of surface crack due to residual copper in carbon steel', Proc. Steelmaking Conf., Vol. 79, 621–626; 1996, Warrendale, PA, ISS.
7. H. Fredricksson, K. Hansson and A. Olsson: *Scand. J. Metall.*, 2001, **30**, 41–50.
8. J. Konishi, M. Militzer, J. K. Brimancombe and I. V. Samarasekera: *Metall. Trans. B*, 2002, **33B**, 413–423.
9. S. Louhenkilpi, J. Miettinen and L. Holappa: *ISIJ Int.*, 2006, **46**, 914–920.
10. R. O. Ritchie and J. F. Knott: 'Effects of fracture mechanisms on fatigue crack propagation', in 'Mechanics and mechanisms of crack growth', 1973, Cambridge, Churchill College, 201-205.
11. V. J. Colangelo and F. A. Heiser: 'Analysis of metallurgical failures', 361; 1974, New York, J. W. and Sons.
12. H. L. Ewalds and R. J. H. Wanhill: 'Fracture mechanics', 304; 1989, London, A. Hode.
13. E. A. López: 'Estudio de la Solidificación de Aceros con Composición Peritéctica', Master thesis, CINVESTAV Unidad Saltillo, Saltillo, México, 2006.
14. H. Mizukami, A. Yamanaka and T. Watanabe: *ISIJ Int.*, 2002, **42**, 964–973.
15. J. M. Ruíz, M. T. Herrera. M. R. Castro and H. T. Solís: *ISIJ Int.*, 2008, **48**, 454–460.
16. DICTRA software: Tool for simulation of diffusional transformations in alloys, 24, Stockholm-Sweden, 2006.
17. W. Clyne and W. Kurz: *Metall. Trans. A*, 1981, **12A**, 965–971.